IEEE Access
Multidisciplinary | Rapid Review | Open Access Journal

Received 15 March 2023, accepted 28 April 2023, date of publication 4 May 2023, date of current version 24 May 2023.

Digital Object Identifier 10.1109/ACCESS.2023.3272905

RESEARCH ARTICLE

Unsupervised Seismic Random Noise Suppression Based on Local Similarity and Replacement Strategy

JIAN GAO[1,2], ZHENCHUN LI[1,2], MIN ZHANG[1,2], YIXUAN GAO[3], AND WANYUE GAO[4]

[1]School of Earth Science and Technology, China University of Petroleum (East China), Qingdao 266500, China
[2]Key Laboratory of Deep Oil and Gas, Qingdao 266500, China
[3]School of Biological Science, Qufu Normal University, Qufu 273165, China
[4]Business School, Shandong Normal University, Jinan 250358, China

Corresponding author: Min Zhang (zhangm@upc.edu.cn)

This work was supported in part by the Major Science and Technology Cooperation Projects of China National Petroleum Corporation under Grant ZD2019-183-003, and in part by the National Natural Science Foundation of China under Grant 42074133.

ABSTRACT Improving the signal-to-noise ratio and suppressing random noise in seismic data is critical for high-precision processing. Although deep learning-based algorithms have gained popularity as denoising methods, they suffer from poor generalization ability, resulting in high training set construction cost and computation cost. To address this problem, we propose an unsupervised learning-based denoising method that includes an improved denoising strategy based on local similarity and replacement, a corresponding training method, and an improved network based on UNet. Our training method takes advantage of network convergence and allows direct training on the test region, effectively solving the problems associated with denoising methods using generalization ability while improving training performance. In addition, our network is specifically designed for the training method and incorporates various improvements that could further enhance the training effectiveness. Our method outperforms traditional denoising methods, as demonstrated by tests on synthetic and field data, with superior performance in random noise attenuation and reflection event reconstruction.

INDEX TERMS Seismic data, random noise, convolutional neural network, unsupervised learning.

I. INTRODUCTION

High precision seismic exploration requires a high signal-to-noise ratio (SNR) of the seismic data as it has a strong influence on the subsequent inversion and geological interpretation of the data [1], [2], [3]. However, noise contamination, which can be mainly categorized as coherent and random noise, is unavoidable during the acquisition process. The latter, random noise, has no fixed frequency or apparent velocity and is usually caused by various types of environmental disturbances during acquisition. This condition results in a significant reduction in the SNR of the seismic data, thus emphasizing the importance of random noise attenuation for SNR improvement.

At present, a variety of noise-reduction methods have been proposed, including F-X deconvolution (FX) [4], [5], t-x domain predictive filtering [6], [7], and their improved methodologies [8], [9], [10]. These methods are based on the principle that seismic effective signals are predictable in the f-x or t-x domain, whereas random noise is unpredictable. By taking advantage of the difference in predictive properties, appropriate filter operators can be designed to suppress random noise in the frequency domain, and the corresponding clean data can be obtained through subsequent inverse transformation. In addition, a growing number of denoising methods that are based on the transform domain have also gained traction. The curvelet transform [11], [12], the wavelet transform [13], [14], the Fourier transform [14], and the seislet transform [15], [16] are some of the most popular methods. These approaches entail transforming the seismic data into a specific transform domain and then

The associate editor coordinating the review of this manuscript and approving it for publication was Fabrizio Marozzo.

This work is licensed under a Creative Commons Attribution-NonCommercial-NoDerivatives 4.0 License.
For more information, see https://creativecommons.org/licenses/by-nc-nd/4.0/

implementing appropriate thresholds, which are designed based on the discernible difference between effective signals and random noise in the transform coefficients, to perform denoising. Despite their effectiveness in attenuating random noise, these transform-domain-based methods often fail to eliminate noise, i.e., they will inevitably mix part of the noise with valid data, resulting in residual noise. Signal processing techniques have witnessed significant advancements in recent years, and decomposition-based algorithms have emerged as a popular approach for noise attenuation and signal reconstruction in seismic data analysis. These algorithms include Empirical Mode Decomposition (EMD) [17], [18], Ensemble EMD (EEMD) [19], [20], Complementary Ensemble EMD (CEEMD) [21], [22], and Variational Mode Decomposition (VMD) [23], [24]. By decomposing the seismic data into several signal components, these methods aim to superimpose the main signal components that represent the clean data, thereby leading to effective signal reconstruction and random noise attenuation. However, the decomposition process can lead to the mixing of clean data and noise, resulting in multiple signal components with unknown mixing ratios, which can cause partial effective signal loss and residual noise in the denoising results. Additionally, rank-reduction methods have also been widely used in noise attenuation tasks, such as Cadzow Filtering [25], Multichannel Singular Spectrum Analysis (MSSA) [26], [27], and Damped MSSA [28], [29]. These methods assume that the ideal clean data can be constructed as a low-rank matrix, and aim to eliminate the rank increased by the random noise in the seismic signal matrix, thereby leading to noise suppression.

In recent years, due to its exceptional performance in processing large amounts of data, the field of machine learning has gained significant attention in various industries [30], [31], [32]. These data-driven processing techniques have become particularly appealing for their novel and efficient processing way to data processing tasks. Among the various machine learning techniques, deep learning-based techniques, especially those employing convolutional neural networks (CNNs), have experienced rapid development. The seismic denoising field has also witnessed the development of these techniques, as multiple denoising methods [33], [34], [35] based on deep learning have been proposed to suppress random noise effectively. Among these methods, the generative adversarial network (GAN) [36], [37], [38], feedforward denoising CNNs (DnCNNs) [39], [40], [41], and their improved methodologies [42], [43], [44] have played an important role in improving the SNR of seismic data and attenuating random noise, thus facilitating subsequent inversion and geological interpretation.

Compared to traditional denoising methods, CNN-based algorithms enable the denoising model to establish nonlinear mappings between noisy data and clean data, thereby achieving random noise attenuation and signal reconstruction [45]. Most methods aim to improve the generalization ability of the denoising model by training on large datasets to enhance denoising performance. However, this characteristic may lead to the following four problems that cannot be ignored. First, the generalization capability of CNNs often performs poorly, thereby restricting their ability to accurately process seismic data. However, the potential convergence ability of CNNs has been largely overlooked and underutilized. Second, under the above training strategy, the inconsistency of the bias degree between the training set and the test set to various geological features may limit the denoising performance to some extent, which imposes higher requirements on the composition cost of the training set. Third, the methods that aim to improve the generalization ability of denoising models require an increase in the diversity of training samples, which in turn significantly heightens the training difficulty of the network. As a result, the acquisition of the desired denoising model necessitates a greater number of training samples and training time. And these together lead to the high computational cost. Finally, repeated training is often employed to evaluate the denoising performance of denoising models, resulting in significant non-negligible training costs, encompassing both the composition cost of the training set and the training time cost. Consequently, reducing the training cost and improving the generalization ability of the network have emerged as two key research areas in this field.

This paper investigates the application of unsupervised deep learning in the context of seismic random noise attenuation, presenting a novel denoising method that comprises an improved denoising strategy and its corresponding training method, as well as an enhanced CNN based on the UNet architecture. We begin by improving the denoising theory proposed by Lehtinen et al. [46] and presenting an improved denoising strategy for seismic random noise suppression. This strategy leverages the local similarity of the data and a replacement-based approach to generate labels for the training set, enabling the labels to be directly derived from the original seismic data. In comparison to deep denoising algorithms that rely on generalization ability, our strategy fully utilizes the convergence ability of the network, effectively addressing the problems faced by such algorithms. We also introduce the corresponding training method aligned with our denoising strategy, along with an improved CNN based on the UNet architecture. This network utilizes the U-shaped processing path, connection layer cancellation, and enhanced feature final processing to optimize the training effect under our proposed method. To assess the effectiveness of our proposed method in random noise attenuation, we applied it to both synthetic and field data. Detailed comparisons were also conducted between our approach and traditional algorithms, including the FX, the MSSA, and the EMD, to evaluate their respective attenuation capabilities. Our experimental results demonstrated that the proposed method outperforms these traditional algorithms in terms of signal reconstruction and noise attenuation.

The rest of this paper is organized as follows. Section II presents the proposed denoising strategy and its

corresponding training method. Section III introduces the improved CNN. In Section IV, experiments are conducted on synthetic and field data to demonstrate the effectiveness of the proposed method in attenuating random noise and reconstructing signals. Finally, Section V concludes this paper.

II. METHODS

A. DENOISING STRATEGY

As we know, the seismic data y can be expressed as follows:

$$y = x + noise \tag{1}$$

where x denotes the clean data; *noise* denotes the Gaussian white noise. To achieve random noise attenuation and effective signal reconstruction, deep learning denoising methods usually take noisy data y and clean data x as input and label of the network, respectively. In this way, the corresponding trained network can have good performance in noise reduction and data reconstruction. The training process is described as follows:

$$\theta_{n2c} = \arg\min_{\theta} \sum_{i} Loss\left(f_{\theta}\left(y_i\right), x_i\right) \tag{2}$$

where θ_{n2c} denotes the parameter of the trained network in the noise-clean training task; (y_i, x_i) denotes a pair of samples of the training set; $f_{\theta}(\cdot)$ denotes the processing of the network using the parameter θ; and *Loss* denotes the loss function. If we use a specific replacement strategy $sim(\cdot)$ for the processing of the seismic data y, we will get the processed noisy data y^{sim} which is described as follows:

$$y^{sim} = sim\left(y\right). \tag{3}$$

Then, we set y and y^{sim} as the input and the label of the network, respectively, and train the network. The corresponding training process can be written as follows:

$$\theta_{n2n} = \arg\min_{\theta} \sum_{i} Loss\left(f_{\theta}\left(y_i\right), y_i^{sim}\right) \tag{4}$$

where θ_{n2n} denotes the parameter of the trained network in the noise-to-noise training task. According to the denoising theory of Lehtinen et al. [46], if the conditional expectation $E\left[y_i^{sim}|y_i\right] = x_i$ is satisfied, the parameter θ_{n2n} can be regarded as equivalent to the parameter θ_{n2c}. In other words, the network using θ_{n2n} can perform as well as θ_{n2c} in random noise suppression. To satisfy the condition, a large number of samples is required. In addition, to make the condition easier to implement, we decompose the condition as follows:

$$\begin{aligned} E\left[y_i^{sim}|y_i\right] &= E\left[x_i^{sim} + noise_i^{sim}|y_i\right] \\ &= E\left[x_i^{sim}|y_i\right] + E\left[noise_i^{sim}|y_i\right] \end{aligned} \tag{5}$$

where x_i^{sim} and $noise_i^{sim}$ denote the clean data and random noise of y_i^{sim}, respectively. In this way, we can use $E\left[x_i^{sim}|y_i\right] = x_i$ and $E\left[noise_i^{sim}|y_i\right] = 0$ to replace the condition. This transformation of the condition can be written as follows:

$$E\left[y_i^{sim}|y_i\right] = x_i \Rightarrow \begin{cases} E\left[x_i^{sim}|y_i\right] = x_i \\ E\left[noise_i^{sim}|y_i\right] = 0 \end{cases}. \tag{6}$$

If y^{sim} processed by $sim(\cdot)$ can satisfy the condition shown in (6), the trained network can have a good performance in random noise attenuation and effective signal construction, as follows:

$$f_{\theta_{n2n}}(y) = f_{\theta_{n2n}}(x + noise) = f_{\theta_{n2c}}(x + noise) \approx x. \tag{7}$$

B. REPLACEMENT STRATEGY

To better satisfy the condition in (6), we use the data replacement method to generate y^{sim}. First, except for the elements in the last row or column of the 2D seismic data, which remain unchanged, all other elements in the matrix are processed individually using a specific replacement method. The processing of the seismic data can be written as follows:

$$y_{m,n}^{sim} = \begin{cases} sim\left(y_{m,n}\right), & m \in [1, M-1], n \in [1, N-1] \\ y_{m,n}, & otherwise \end{cases} \tag{8}$$

where M and N denote the dimensions of the seismic gather. For each element $y_{m,n} (m \in [1, M-1]; n \in [1, N-1])$ to be replaced, a 2×2 matrix $Y^{m,n} = \begin{bmatrix} y_{m,n} & y_{m,n+1} \\ y_{m+1,n} & y_{m+1,n+1} \end{bmatrix} (m \in [1, M-1]; n \in [1, N-1])$ is constructed with the element $y_{m,n}$ in the upper left corner. Use this matrix $Y^{m,n}$ and all other 2×2 matrices $Y^{i,j} = \begin{bmatrix} y_{i,j} & y_{i,j+1} \\ y_{i+1,j} & y_{i+1,j+1} \end{bmatrix} (i \neq m; j \neq n)$ in the seismic data for similarity comparison, and obtain the matrix $\hat{A}^{m,n}$ with the highest similarity. Then randomly select an element from the matrix $\hat{A}^{m,n}$ as the replacement element $\hat{a}^{m,n}$ of $y_{m,n}$, as follows:

$$\hat{a}^{m,n} = rand\left(\hat{A}^{m,n}\right) \tag{9}$$

where $rand(\cdot)$ stands for randomly returning an element from the matrix. Note that the elements $y_{m,n}$ in y are not changed during the replacement process, and the obtained replacement elements $\hat{a}^{m,n}$ would replace $y_{m,n}$ in the end of the process, thereby leading to a new matrix $\hat{y}$, as follows:

$$\hat{y}_{m,n} = \begin{cases} \hat{a}^{m,n}, & m \in [1, M-1], n \in [1, N-1] \\ y_{m,n}, & otherwise. \end{cases} \tag{10}$$

It is also important to note that the vast majority of reflection events in $\hat{y}$ after the replacement processing present polarity reversal. In order to ensure that the condition $\begin{cases} E\left[x_i^{sim}|y_i\right] = x_i \\ E\left[noise_i^{sim}|y_i\right] = 0 \end{cases}$ of (6) is satisfied, we will perform additional processing on $\hat{y}$ by (11) to generate y^{sim}. Equation (11) is expressed as follows:

$$y_{m,n}^{sim} = \frac{1}{2}\left(\frac{3y_{m,n} - \hat{y}_{m,n}}{2}\right). \tag{11}$$

In this way, we consider that the condition $E\left[x_i^{sim}|y_i\right] = x_i$ is satisfied. Assessing the presence of large-scale polarity reversal amidst the random noise in $\hat{y}$ is challenging. Nonetheless, given that random noise is typically considered to be Gaussian white noise, we can assume that any polarity reversal would have a negligible effect on the random noise. In other words, the random noise in $\hat{y}$ can be considered unchanged regardless of the polarity reversal, as follows:

$$noise_{m,n} = \hat{n}_{m,n} \tag{12}$$

where $\hat{n}_{m,n}$ denotes the random noise of $\hat{y}_{m,n}$. This also means that the amplitude of the random noise in y^{sim} would be halved after the processing shown in (11), as follows:

$$noise_{m,n}^{sim} = \frac{1}{2}\left(\frac{3noise_{m,n} - \hat{n}_{m,n}}{2}\right) = \frac{1}{2}noise_{m,n}. \tag{13}$$

Although the amplitude of the random noise changes, considering that the random noise is Gaussian white noise, the processed $noise^{sim}$ still satisfies the condition $E\left[noise_i^{sim}|y_i\right] = 0$.

C. SIMILARITY CALCULATION

We adopt Bray-Curtis distance [47], [48] to evaluate the similarity between $Y^{m,n}$ and $Y^{i,j}$. The distance can be written as follows:

$$Dist(A, B) = \frac{\sum_{i=1}^{R}\sum_{j=1}^{C}\left|A_{ij} - B_{ij}\right|}{\sum_{i=1}^{R}\sum_{j=1}^{C}A_{ij} + \sum_{i=1}^{R}\sum_{j=1}^{C}B_{ij}} \tag{14}$$

where $Dist\,(A, B)$ represents the Bray-Curtis distance between the matrix A and the matrix B; R and C denote the number of rows and columns of the matrix, respectively. By computing the dissimilarity between the elements of the matrix relative to their sum, the Bray-Curtis distance effectively constrains the distance metric to a smaller range. Consequently, this feature makes the Bray-Curtis distance more robust to outliers than the conventional Euclidean distance for matrix similarity calculations.

D. TRAINING METHOD

Based on the denoising strategy proposed above, we propose the corresponding training method as shown in Fig. 1. The training method can be described in detail as follows:

Step 1: Select a raw seismic data y for noise attenuation. Then process y with the specific replacement strategy to get y^{sim}.

Step 2: Generate a set of positions ($[pos_1, pos_2, \ldots, pos_n]$) to compose a position sequence S_{pos} by randomly selecting in y, where $S_{pos} = [pos_1, pos_2, \ldots, pos_n]$, and n is the number of samples in the training set. According to each position $pos_i\,(i \in [1, n])$ in the position sequence S_{pos}, generate the corresponding 64×64 patches ($P_i^y\,(i \in [1, n])$ and $P_i^{y^{sim}}\,(i \in [1, n])$) from the two data ($y$ and y^{sim}), and compose these two patches as a training sample $ts_i\,(i \in [1, n])$.

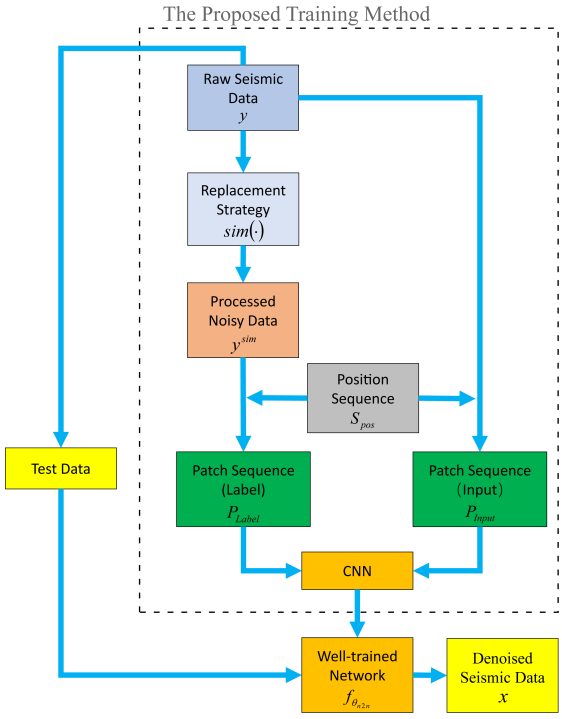

FIGURE 1. Random noise attenuation process based on the improved CNN.

Step 3: Compose the training samples ($ts_i\,(i \in [1, n])$) obtained in step. 2 as a training set. The training set can be divided into two parts, i.e., the input patch sequence $P_{Input} = \left[P_1^y, P_2^y, \ldots, P_n^y\right]$ and the label patch sequence $P_{Label} = \left[P_1^{y^{sim}}, P_2^{y^{sim}}, \ldots, P_n^{y^{sim}}\right]$.

Step 4: The sequences (P_{Input} and P_{Label}) are used as the input and label of the network, respectively. Train the network and stop training at the appropriate epoch to get the well-trained network.

The mean square error (MSE) is a commonly employed metric to evaluate the effectiveness of network training. In this study, the loss function can be expressed as follows:

$$L\,(\theta) = \frac{1}{2W}\sum_{i=1}^{W}\left\|f_\theta\,(y_i) - y_i^{sim}\right\|_F^2 \tag{15}$$

where W represents the number of samples in the training set; $\|\cdot\|_F$ represents the Frobenius norm.

From the perspective of training strategy, the proposed method has an obvious advantage over the denoising methods based on generalization ability. Specifically, this method can construct a training set directly from the original data, instead of constructing a training set with similar seismic properties in accordance with the characteristics of the original data. It can free us from the problem of limiting the denoising performance due to the inconsistency of the degree of bias between the training set and the test set to different geological features. This results in lower requirements and costs for the training set construction.

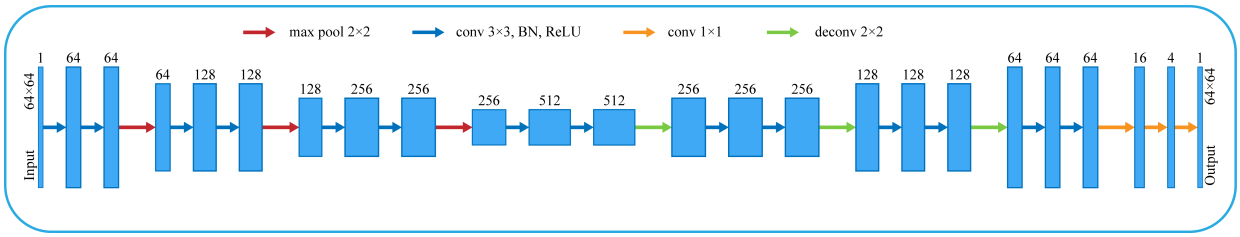

FIGURE 2. Architecture of the improved CNN.

III. OUR CNN ARCHITECTURE FOR SEISMIC DENOISING

In pursuit of superior performance in random noise suppression and signal reconstruction, we engineered an upgraded end-to-end convolutional neural network (CNN) based on UNet [49], as shown in Fig. 2. Under the proposed training method, the highest-level features primarily comprise the features of the valid data. Simultaneously, the lower the feature level, the higher the proportion of features from random noise. Consequently, to effectively utilize the high-level features and enhance the performance of the trained network, the CNN employs a U-shaped processing path similar to that of UNet. Note that the CNN cancels the concatenation layers, resulting in a strong bias towards the highest-level features in the network's output. This mechanism holds promise for improving denoising performance. The encoding process of the CNN involves a series of layers including convolution layers (conv), rectified linear unit layers (ReLU), batch normalization layers (BN), and max-pooling layers (max pool). In the corresponding decoding process, the conv, the ReLU, the BN, and the deconvolution layers (deconv) are utilized for data reconstruction. Different from the processing module employed in UNet, i.e., conv+ReLU, our CNN utilizes conv+BN+ReLU as the processing module for each feature map. The BN can suppress the offset of the covariant [50] to some extent to reduce its bad impact on the network training efficiency. Simultaneously, the BN can also decrease overfitting to a certain extent. Overfitting occurs when a network "memorizes" the training data instead of learning general features that allow it to make accurate predictions on new data. To prevent overfitting and promote generalization, it is crucial to employ the BN. Furthermore, the BN can address the problem of gradient vanishing that often arises during network training, while the activation function used in conjunction with BN can effectively prevent gradient explosion.

In addition, a common practice in feature map processing is to insert a 1×1 convolutional layer at the end of the network, which is intended to transform the multi-channel feature map into a single-channel feature map [51], [52]. In our CNN, we replace this 1×1 conv with a processing module, i.e., multiple 1×1 conv, to achieve better denoising performance. The number of filters in each 1×1 conv is successively reduced from the anterior to the posterior layers until it reaches a single filter. Compared to using only a single convolutional layer, the selection of this processing module offers the following advantages: (1) the module with a gradually decreasing number of filters can preserve the features obtained by the CNN as much as possible, thereby reducing the degree of feature loss after the convolution operations; (2) the transformation plays a more important role in network training. The module can increase the number of selectable parameters and expand the selected parameter range. This enhances the resilience of the module to parameter selection, thus promoting feature learning by the network. In addition, the improvement of the network learning ability means the improvement of the network utilization rate to samples in the training set. This results in an effective reduction in the number of samples required to achieve a denoising effect. In this paper, the processing module is composed of three 1×1 conv, whose convolutional kernel sizes are set to 16, 4, and 1 in order from the front to the back.

IV. NUMERICAL RESULTS

In this section, we begin by introducing the evaluation metrics utilized in our experiments. Subsequently, we outline the hyperparameter configurations employed during training. Finally, we apply the trained denoising model to both synthetic and field data. All experiments were conducted on a PC with an Intel Core i5-12400F 2.50 GHz CPU, 16 GB of memory, and an NVIDIA GeForce RTX 3060 GPU.

A. DATA ANALYSIS

To quantitatively evaluate the denoising performance of various methods, we employed the signal-to-noise ratio (SNR) [53] as a metric for assessing the denoised results. The SNR is a widely adopted indicator for evaluating the efficacy of denoising methods, measuring the ratio of signal power to noise power in a given dataset. A higher SNR value usually indicates superior denoising performance. Mathematically, the SNR is expressed as follows:

$$SNR = 10\log_{10}\frac{\|x\|_2^2}{\|x-\hat{x}\|_2^2} \tag{16}$$

where $\hat{x}$ and x represent the denoising result and the clean data from the noisy data, respectively.

B. HYPERPARAMETER SETTING

This study employed the following hyperparameter settings for training: first, the Adam optimizer was selected as the solver. This widely used solver dynamically adjusts the learning rate and utilizes momentum to prevent the network from

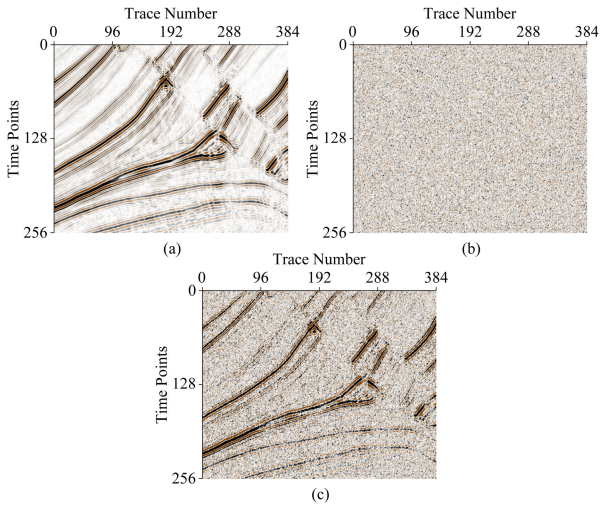

FIGURE 3. Synthetic example. (a) Clean data. (b) Random noise. (c) Noisy data.

getting trapped in suboptimal solutions with limited generalization. Moreover, the Adam optimizer's oscillation reduction feature enhances the noise suppression effectiveness of the denoising model. The initial learning rate was set to 0.001, and a batch size of 32 was chosen. The smaller batch size has a positive impact on training accuracy, while the choice of a batch size that is a multiple of 8 aligns with computer hardware data storage, thereby reducing the time cost of accessing data and ultimately improving the training speed of the network. For patch size, we opted for 64×64, which has been widely used in previous works and balances computational complexity with spatial resolution. Finally, the network was trained for 38 epochs to ensure convergence to a stable solution.

In summary, the hyperparameters chosen in this study have been demonstrated to be effective. These choices enhance the denoising model's robustness to noisy input data, accuracy, and computational efficiency.

C. EXPERIMENTS ON SYNTHETIC DATA

To demonstrate the exceptional performance of our proposed method in suppressing random noise, we conducted experiments on a section of the post-stack data from the Marmousi2 model [54]. This particular area, shown in Fig. 3(a), is comprised of 384 traces and 256 sampling points and features two substantial faults, a portion of a salt mound, and a segment of an anomalous body with both high and low velocity. As a result, this region contains a diverse range of reflection events that serve to comprehensively evaluate denoising methods. To generate synthetic noisy data for testing purposes, we added 0dB Gaussian white noise to the region, which is shown in Fig. 3(b), while the resulting noisy data is presented in Fig. 3(c). It is evident that due to the presence of random noise, the significance and coherence of the reflection events' amplitude in the noisy data were lost to varying degrees.

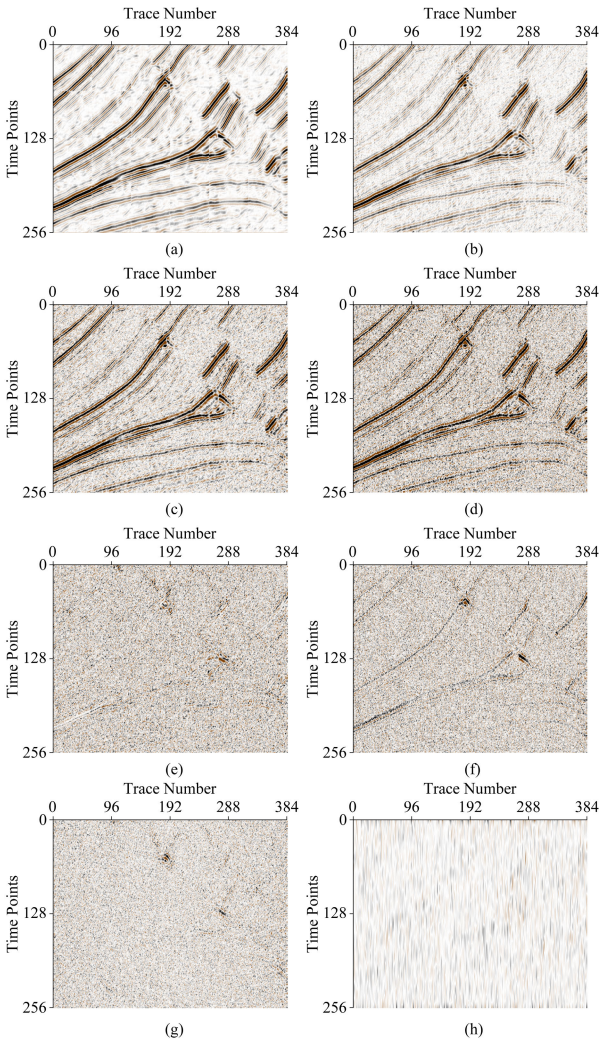

FIGURE 4. Comparisons for denoising results and removed noise. Denoising results: (a) CNN (19.25dB); (b) FX (4.42dB); (c) MSSA (4.62dB); (d) EMD (3.14dB). Removed noise: (e) CNN; (f) FX; (g) MSSA; (h) EMD.

We created a training set comprising 384 samples and a test set from this region, evaluating the efficacy of the proposed method. As shown in Fig. 4(a), our proposed method achieved a denoising result with an SNR of 19.25 dB. The corresponding loss curve is exhibited in Fig. 5(b), and the training time totaled 97 seconds. We can observe that our approach successfully attenuated the most of random noise present in the denoising result, and reconstructed part weak reflections previously covered by the noise. Notely, the proposed method performed with high denoising proficiency, despite the presence of complex geological structures such as faults in the test region. To better demonstrate the effectiveness of the proposed method, we evaluated the FX, the MSSA, and the EMD on the synthetic data. Compared with our proposed method, the denoising results of the FX, the MSSA, and the EMD showed obvious random noise pollution, with SNRs of 4.42 dB, 4.62 dB, and 3.14 dB, respectively (Fig. 4(b)-(d)). Among the three methods, the EMD incurred the most severe

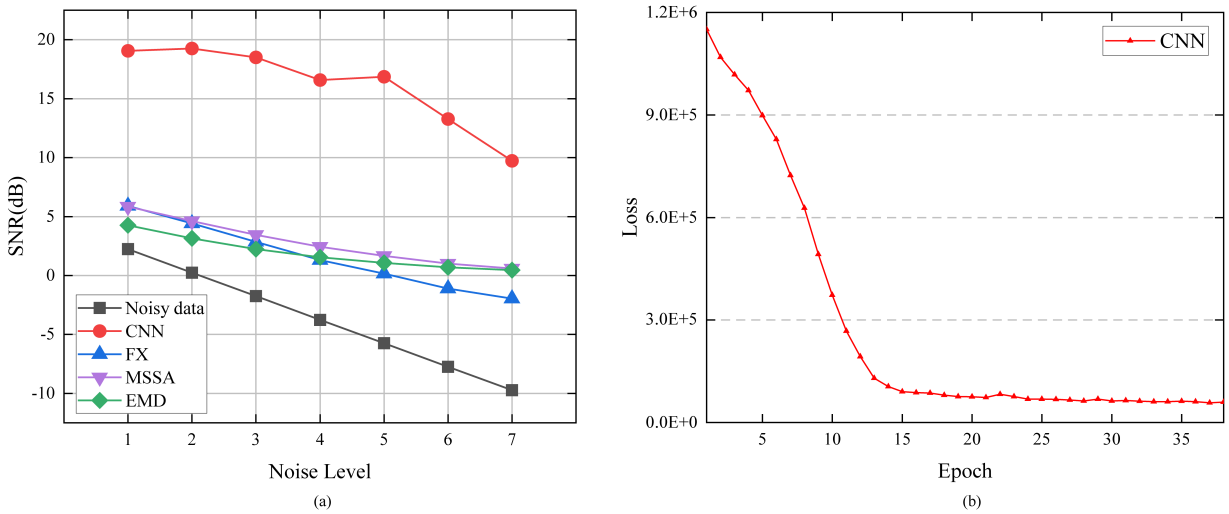

FIGURE 5. SNR comparison at different noise levels and training loss in different epochs. (a) SNR comparison of CNN, FX, MSSA, and EMD. (b) Training loss of CNN.

noise pollution, followed by the MSSA. Comparatively, the denoising result of the FX was better, but some slight noise persisted. The corresponding noise profiles for the methods are shown in Fig. 4(e)-(h). We can observe that the profile from the proposed method had some slight continuous reflection signals, indicating that our approach caused a minor loss of effective signals. However, the degree of loss was less than that incurred by the MSSA (Fig. 4(g)) but greater than that of the FX (Fig. 4(f)).

In addition, we applied these methods to the synthetic data with seven different levels of random noise and analyzed the SNR of their denoising results, as shown in Fig. 5(a). The red line corresponds to the proposed method, and the black line denotes the noisy data. The blue, purple, and green lines represent the FX, the MSSA, and the EMD, respectively. We can observe that the proposed method consistently achieved a significantly higher SNR than the other methods across all noise levels. Notably, the SNRs of the FX, the MSSA, and the EMD were very close at each noise level, with a maximum difference of only 2.5 dB.

To further investigate the effectiveness of the proposed denoising method, we conducted a comparative analysis of the FK spectra of the denoising profiles using different approaches, as shown in Fig. 6. The FK spectra of the noisy data and the clean data are shown in Fig. 6(a) and Fig. 6(b), respectively. Fig. 6(d) reveals that the FK spectrum obtained by the FX contained significant low-energy noise in the entire frequency and wavenumber domains, especially in the 16-35 Hz range. Moreover, there was also a discernible energy loss in the effective signals, indicating that the FX did not perform well in random noise suppression. The FK spectrum of the MSSA, as shown in Fig. 6(e), revealed no residual random noise only in the 10-40 Hz range, and the valid data also experienced severe energy loss similar to that observed in the FX, with only weak signals exhibiting less energy loss than those from the FX. Additionally, the FK

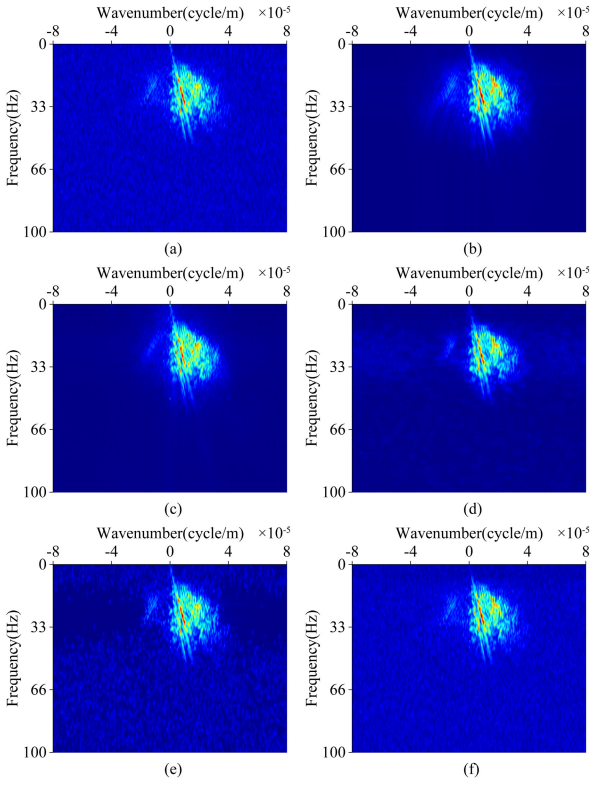

FIGURE 6. F-K domain analysis for the processing results. (a) Noisy data. (b) Clean data. (c)-(f) Denoising results for CNN, FX, MSSA, and EMD, respectively.

spectrum of the EMD is shown in Fig. 6(f). We can observe that the valid data suffered from the same level of energy loss as observed in the MSSA, and the residual noise was even more apparent than that in the FX and the MSSA. In contrast, as shown in Fig. 6(c), our proposed method could eliminate random noise obviously while retaining the reflection events

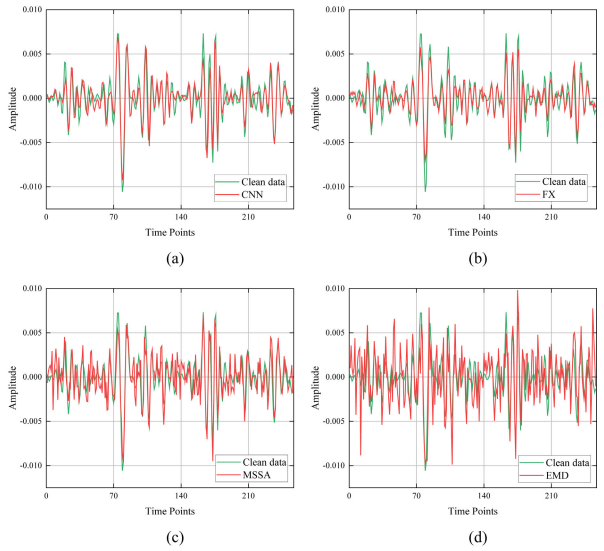

FIGURE 7. Amplitude comparisons for the 155th trace record. (a) CNN. (b) FX. (c) MSSA. (d) EMD.

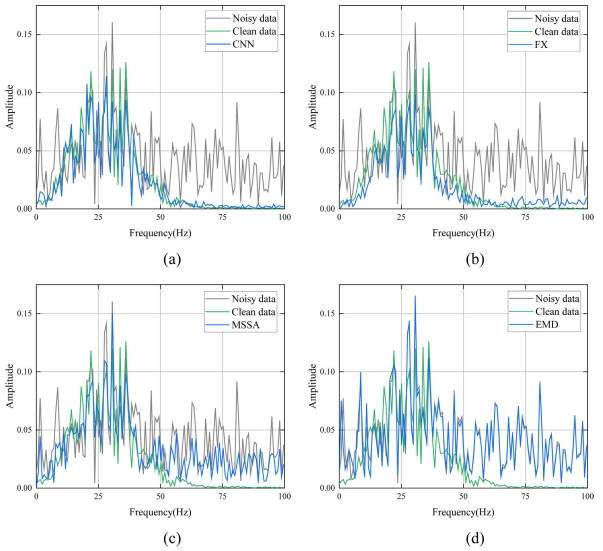

FIGURE 8. Spectral comparisons for the 155th trace record. (a) CNN. (b) FX. (c) MSSA. (d) EMD.

effectively, as its FK spectrum was highly similar to that from the clean data.

The effectiveness of the proposed denoising method in preserving the amplitude and frequency characteristics of seismic data was evaluated through amplitude and spectral comparisons. To perform the analysis, the 155th trace of the synthetic data was selected as the test trace. The respective amplitudes of the clean data, the noisy data, and the denoising results from the proposed approach as well as three other methods (the FX, the MSSA, and the EMD) were compared in Fig. 7. The results reveal that the denoising waveforms obtained from the proposed method presented greater resemblance to the original clean waveforms than those from the other three methods. To further evaluate the performance of the proposed method, the frequency spectrums of the denoising data from the methods were also compared. As shown in Fig. 8, the proposed approach surpassed the other three methods in suppressing random noise and reconstructing effective signals, especially for frequency components ranging from 50 to 100 Hz. These findings demonstrate the effectiveness of the proposed method in attenuating random noise while preserving the amplitude and frequency features of the original clean data.

D. EXPERIMENTS ON FIELD DATA

In the process of denoising field data, the identification of complex and uncertain factors, such as the noise level and the velocity field, is a challenging task. As a result, the performance of traditional denoising methods often falls short of expectations. To further demonstrate the effectiveness of our proposed approach, we have selected a region consisting of 384 traces and 256 sampling points from marine seismic data (http://cotuit.er.usgs.gov/Data/1978-015-FA/SE/001/38/) for testing, as shown in Fig. 9. We constructed a training set of

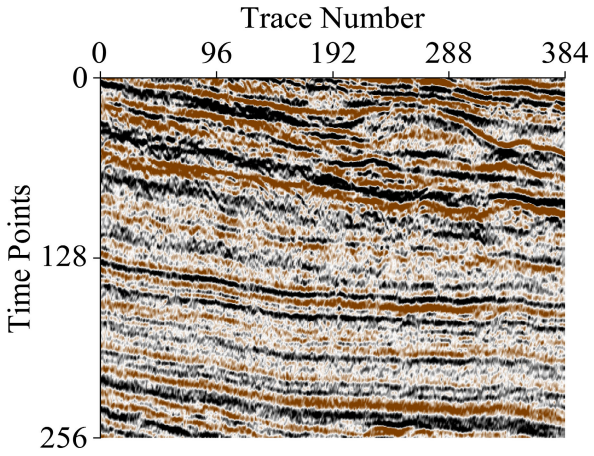

FIGURE 9. The field seismic data.

384 samples from this region, and the training time was 97 s. The denoising results obtained from the CNN, the FX, the MSSA, and the EMD are shown in Fig. 10(a)-(d), and the corresponding noise profiles are shown in Fig. 10(i)-(l). As a whole, the CNN, the FX, and the MSSA were effective in attenuating the random noise and reconstructing the reflection events, whereas the EMD retained a certain amount of noise.

To better demonstrate the attenuation capacity of the proposed method, we conducted an experiment using a 64×64 zoomed-in portion of the field data, as shown in Fig. 10(e)-(h). By zooming in, we are able to discern intricate details of the seismic profiles and observe the differences between the results obtained from different methods in more detail. The seismic profile processed by our proposed method exhibited clear reconstruction of reflection events, with almost complete attenuation of random noise, leading

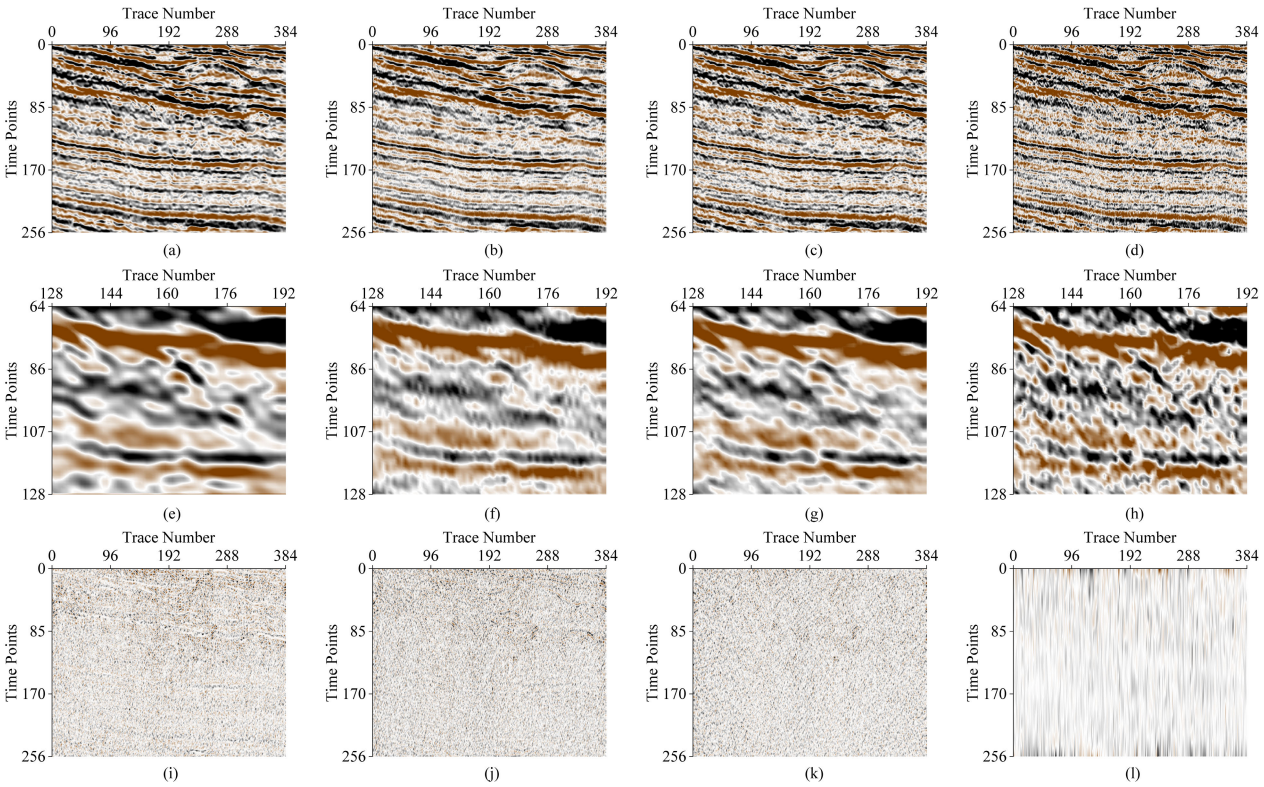

FIGURE 10. Denoising performances of field seismic data. Denoising results: (a) CNN; (b) FX; (C) MSSA; (d) EMD. Zoomed-in portion of field data: (e) CNN; (f) FX; (g) MSSA; (h) EMD. Removed noise: (i) CNN; (j) FX; (k) MSSA; (l) EMD.

to a more precise and accurate presentation of the subsurface structure. Although the FX was able to reconstruct reflection events effectively, it left behind a small amount of noise compared to our proposed method. Such residual noise could cause difficulties in interpreting and analyzing the seismic data, thereby affecting the overall accuracy of the subsurface model. Similarly, the MSSA was able to reconstruct effective signals, but the residual noise in the denoising result was more obvious than the FX. In contrast, the EMD failed to completely reconstruct the reflection events, leaving noticeable noise that could significantly affect the interpretation and analysis of the seismic data. Overall, these comparisons demonstrate that our proposed method outperformed the FX, the MSSA, and the EMD in terms of noise reduction and reconstruction of reflection events in the subsurface structure.

V. CONCLUSION

In this study, we present an improved method for attenuating seismic random noise based on unsupervised learning. Our proposed method includes an improved denoising strategy that utilizes the local similarity of the data and the replacement strategy, along with its corresponding training method and an improved CNN based on UNet. Specifically, our denoising strategy utilizes local similarity to identify the most similar part for each element in the matrix and obtains the replacement elements from these similar parts using the replacement strategy. These replacement elements would then replace the original element to construct a new matrix, which serves as the label of the training set. This novel approach allows the corresponding training method to generate training labels directly from the test region, thus overcoming the limitations of denoising methods that rely solely on generalization capability and presenting better training performance. Furthermore, we propose an improved CNN based on UNet, which is specifically designed for the training method to improve the training effect. In the proposed CNN, the improvement in output bias for different level features can effectively enhance denoising performance. Additionally, the improvement in the final processing of feature maps can effectively increase the utilization rate of samples in the training set, resulting in a reduction of the number of samples needed to achieve a denoising effect. Our experimental results on synthetic and field data demonstrate that our proposed method outperforms traditional denoising methods, showing excellent performance in random noise attenuation and seismic signal reconstruction. However, we note that the denoising ability of our proposed method may degrade under extremely low signal-to-noise ratio (SNR) conditions. Moreover, the reasons for the polarity reversal of most reflection events after the replacement processing remain unknown and require further investigation. Despite these limitations, our proposed method has promising applications in complex random noise attenuation and seismic signal processing.

ACKNOWLEDGMENT

The authors would like to thank the reviewers and the journal's editors. Comments by the journal's editors and the associated reviewers are very helpful in improving the manuscript.

REFERENCES

[1] G. Li, Y. Li, and B. Yang, "Seismic exploration random noise on land: Modeling and application to noise suppression," *IEEE Trans. Geosci. Remote Sens.*, vol. 55, no. 8, pp. 4668–4681, Aug. 2017.

[2] W. Sun, Z. Li, and Y. Qu, "The 3D conical radon transform for seismic signal processing," *Geophysics*, vol. 87, no. 5, pp. 481–504, Sep. 2022.

[3] G.-H. Li and Y. Li, "Random noise of seismic exploration in desert modeling and its applying in noise attenuation," *Chin. J. Geophys.*, vol. 59, no. 2, pp. 682–692, 2016.

[4] L. L. Canales, "Random noise reduction," in *Proc. SEG Tech. Program Expanded Abstr.*, 1984, pp. 525–527.

[5] D. Bonar and M. Sacchi, "Spectral decomposition with f-x-y preconditioning," *Geophys. Prospecting*, vol. 61, pp. 152–165, Jun. 2013.

[6] J. F. Claerbout and R. Abma, *Earth Soundings Analysis: Processing Versus Inversion*, vol. 6. London, U.K.: Blackwell Scientific, 1992.

[7] Y. Liu and B. Li, "Streaming orthogonal prediction filter in the t-x domain for random noise attenuation," *Geophysics*, vol. 83, no. 4, pp. 41–48, Jul. 2018.

[8] G. Liu, X. Chen, J. Du, and K. Wu, "Random noise attenuation using f-x regularized nonstationary autoregression," *Geophysics*, vol. 77, no. 2, pp. 61–69, Mar. 2012.

[9] S. Fomel and J. Claerbout, "Streaming prediction-error filters," in *Proc. SEG Int. Expo. Annu. Meeting*, 2016, pp. 4787–4791.

[10] M. Naghizadeh and M. Sacchi, "Multicomponent f-x seismic random noise attenuation via vector autoregressive operators," *Geophysics*, vol. 77, no. 2, pp. 91–99, Mar. 2012.

[11] W. Liu, S. Cao, Y. Chen, and S. Zu, "An effective approach to attenuate random noise based on compressive sensing and curvelet transform," *J. Geophys. Eng.*, vol. 13, no. 2, pp. 135–145, 2016.

[12] H. Zhang, H. Yang, G. Huang, Z. Ding, and H. Li, "Random noise attenuation of non-uniformly sampled 3D seismic data along two spatial coordinates using non-equispaced curvelet transform," *J. Appl. Geophys.*, vol. 151, no. 4, pp. 221–233, 2018.

[13] Y. Chen, "Dip-separated structural filtering using seislet transform and adaptive empirical mode decomposition based dip filter," *Geophys. J. Int.*, vol. 206, no. 1, pp. 457–469, 2016.

[14] S. M. Mousavi, C. A. Langston, and S. P. Horton, "Automatic microseismic denoising and onset detection using the synchrosqueezed continuous wavelet transform," *Geophysics*, vol. 81, no. 4, pp. 341–355, Jul. 2016.

[15] Y. Chen and S. Fomel, "EMD-seislet transform," *Geophysics*, vol. 83, no. 1, pp. 27–32, Jan. 2018.

[16] S. Fomel and Y. Liu, "Seislet transform and seislet frame," *Geophysics*, vol. 75, no. 3, pp. 25–38, May 2010.

[17] M. Bekara and M. van der Baan, "Random and coherent noise attenuation by empirical mode decomposition," *Geophysics*, vol. 74, no. 5, pp. 89–98, Sep. 2009.

[18] J. P. A. Sanchez, O. C. Alegria, M. V. Rodriguez, J. A. L. C. Abeyro, J. R. M. Almaraz, and A. D. Gonzalez, "Detection of ULF geomagnetic anomalies associated to seismic activity using EMD method and fractal dimension theory," *IEEE Latin Amer. Trans.*, vol. 15, no. 2, pp. 197–205, Feb. 2017.

[19] W. Huang, R. Wang, S. Zu, and Y. Chen, "Low-frequency noise attenuation in seismic and microseismic data using mathematical morphological filtering," *Geophys. J. Int.*, vol. 211, no. 3, pp. 1296–1318, Dec. 2017.

[20] Z. Wu and N. E. Huang, "Ensemble empirical mode decomposition: A noise-assisted data analysis method," *Adv. Adapt. Data Anal.*, vol. 1, no. 1, pp. 1–41, 2009.

[21] J. R. Yeh, J. S. Shieh, and N. E. Huang, "Complementary ensemble empirical mode decomposition: A novel noise enhanced data analysis method," *Adv. Adapt. Data Anal.*, vol. 2, no. 2, pp. 135–156, 2010.

[22] L. Dong, D. Wang, Y. Zhang, and D. Zhou, "Signal enhancement based on complex curvelet transform and complementary ensemble empirical mode decomposition," *J. Appl. Geophys.*, vol. 144, pp. 144–150, Sep. 2017.

[23] K. Dragomiretskiy and D. Zosso, "Variational mode decomposition," *IEEE Trans. Signal Process.*, vol. 62, no. 3, pp. 531–544, Feb. 2014.

[24] W. Liu, S. Cao, and Z. Wang, "Application of variational mode decomposition to seismic random noise reduction," *J. Geophys. Eng.*, vol. 14, no. 4, p. 888, 2017.

[25] S. Trickett, L. Burroughs, and A. Milton, "Robust rank-reduction filtering for erratic noise," in *Proc. SEG Annu. Meeting*, Sep. 2012, pp. 1–5.

[26] V. Oropeza and M. Sacchi, "Simultaneous seismic data denoising and reconstruction via multichannel singular spectrum analysis," *Geophysics*, vol. 76, no. 3, pp. 25–32, May 2011.

[27] Y. Zhang, H. Zhang, Y. Yang, N. Liu, and J. Gao, "Seismic random noise separation and attenuation based on MVMD and MSSA," *IEEE Trans. Geosci. Remote Sens.*, vol. 60, 2022, Art. no. 5908916.

[28] W. Huang, R. Wang, Y. Chen, H. Li, and S. Gan, "Damped multichannel singular spectrum analysis for 3D random noise attenuation," *Geophysics*, vol. 81, no. 4, pp. 261–270, Jul. 2016.

[29] Y. Chen, D. Zhang, Z. Jin, X. Chen, S. Zu, W. Huang, and S. Gan, "Simultaneous denoising and reconstruction of 5-D seismic data via damped rank-reduction method," *Geophys. J. Int.*, vol. 206, no. 3, pp. 1695–1717, 2016.

[30] M. I. Jordan and T. M. Mitchell, "Machine learning: Trends, perspectives, and prospects," *Science*, vol. 349, no. 6245, pp. 255–260, 2015.

[31] B. Mahesh, "Machine learning algorithms—A review," *Int. J. Sci. Res.*, vol. 9, pp. 381–386, Jan. 2020.

[32] J. Wei, X. Chu, X.-Y. Sun, K. Xu, H.-X. Deng, J. Chen, Z. Wei, and M. Lei, "Machine learning in materials science," *InfoMat*, vol. 1, no. 3, pp. 338–358, 2019.

[33] S. Yu, J. Ma, and W. Wang, "Deep learning for denoisingdeep learning for denoising," *Geophysics*, vol. 84, no. 6, pp. 333–350, 2019.

[34] D. Liu, W. Wang, W. Chen, X. Wang, Y. Zhou, and Z. Shi, "Random-noise suppression in seismic data: What can deep learning do?" in *Proc. SEG Int. Expo. Annu. Meeting*, Aug. 2018, pp. 2016–2020.

[35] W. Li, H. Liu, and J. Wang, "A deep learning method for denoising based on a fast and flexible convolutional neural network," *IEEE Trans. Geosci. Remote Sens.*, vol. 60, 2022, Art. no. 5902813.

[36] H. Wang, Y. Li, and X. Dong, "Generative adversarial network for desert seismic data denoising," *IEEE Trans. Geosci. Remote Sens.*, vol. 59, no. 8, pp. 7062–7075, Nov. 2020.

[37] X. Dong and Y. Li, "Denoising the optical fiber seismic data by using convolutional adversarial network based on loss balance," *IEEE Trans. Geosci. Remote Sens.*, vol. 59, no. 12, pp. 10544–10554, Dec. 2021.

[38] H. Ma, Y. Sun, N. Wu, and Y. Li, "Relative attributes-based generative adversarial network for desert seismic noise suppression," *IEEE Geosci. Remote Sens. Lett.*, vol. 19, pp. 1–5, 2021.

[39] Y. Zhao, Y. Li, X. Dong, and B. Yang, "Low-frequency noise suppression method based on improved DnCNN in desert seismic data," *IEEE Geosci. Remote Sens. Lett.*, vol. 16, no. 5, pp. 811–815, May 2019.

[40] T. Zhong, M. Cheng, X. Dong, and N. Wu, "Seismic random noise attenuation by applying multiscale denoising convolutional neural network," *IEEE Trans. Geosci. Remote Sens.*, vol. 60, 2022, Art. no. 5905013.

[41] H. Ma, Y. Wang, Y. Li, and Y. Zhao, "Desert seismic low-frequency noise attenuation using low-rank decomposition-based denoising convolutional neural network," *IEEE Trans. Geosci. Remote Sens.*, vol. 60, 2022, Art. no. 5900809.

[42] W. Zhu, A. C. Bovik, S. M. Mousavi, and G. C. Beroza, "Seismic signal denoising and decomposition using deep neural networks," *IEEE Trans. Geosci. Remote Sens.*, vol. 57, no. 11, pp. 9476–9488, Aug. 2019.

[43] W. Fang, L. Fu, and H. Li, "Unsupervised CNN based on self-similarity for seismic data denoising," *IEEE Geosci. Remote Sens. Lett.*, vol. 19, pp. 1–5, 2022.

[44] H. Lin, S. Wang, and Y. Li, "A branch construction-based CNN denoiser for desert seismic data," *IEEE Geosci. Remote Sens. Lett.*, vol. 18, no. 4, pp. 736–740, Apr. 2021.

[45] Y. Li, H. Wang, and X. Dong, "The denoising of desert seismic data based on cycle-GAN with unpaired data training," *IEEE Geosci. Remote Sens. Lett.*, vol. 18, no. 11, pp. 2016–2020, Nov. 2020.

[46] J. Lehtinen, J. Munkberg, J. Hasselgren, S. Laine, T. Karras, M. Aittala, and T. Aila, "Noise2Noise: Learning image restoration without clean data," 2018, *arXiv:1803.04189*.

[47] H. G. Gauch, "A quantitative evaluation of the Bray–Curtis ordination," *Ecology*, vol. 54, no. 4, pp. 829–836, Jul. 1973.

[48] E. W. Beals, "Bray–Curtis ordination: An effective strategy for analysis of multivariate ecological data," in *Advances in Ecological Research*, vol. 14. Amsterdam, The Netherlands: Elsevier, 1984, pp. 1–55.

[49] O. Ronneberger, P. Fischer, and T. Brox, "U-Net: Convolutional networks for biomedical image segmentation," in *Proc. Int. Conf. Med. Image Comput. Comput.-Assist. Intervent.* Cham, Switzerland: Springer, 2015, pp. 234–241.
[50] V. López, A. Fernández, and F. Herrera, "On the importance of the validation technique for classification with imbalanced datasets: Addressing covariate shift when data is skewed," *Inf. Sci.*, vol. 257, pp. 1–13, Feb. 2014.
[51] L. Yang, W. Chen, H. Wang, and Y. Chen, "Deep learning seismic random noise attenuation via improved residual convolutional neural network," *IEEE Trans. Geosci. Remote Sens.*, vol. 59, pp. 7968–7981, 2021.
[52] T. Zhong, M. Cheng, X. Dong, Y. Li, and N. Wu, "Seismic random noise suppression by using deep residual U-Net," *J. Petroleum Sci. Eng.*, vol. 209, Feb. 2022, Art. no. 109901.
[53] W. Li and J. Wang, "Residual learning of cycle-GAN for seismic data denoising," *IEEE Access*, vol. 9, pp. 11585–11597, 2021.
[54] G. S. Martin, K. J. Marfurt, and S. Larsen, "Marmousi-2: An updated model for the investigation of AVO in structurally complex areas," in *Proc. SEG Annu. Meeting*, Jan. 2002, pp. 1979–1982.

JIAN GAO received the B.S. degree in transportation from Inner Mongolia University, Huhhot, China, in 2020. He is currently pursuing the M.S. degree in geophysics with the China University of Petroleum (East China).

His research interests include deep learning, swarm intelligence, and seismic data denoising and reconstruction.

ZHENCHUN LI received the B.S. and M.S. degrees in geophysics from the China University of Petroleum (East China), Qingdao, China, in 1983 and 1991, respectively, and the Ph.D. degree in geophysics from Tongji University, Shanghai, China, in 2002.

He is currently the Director of SWPI, China University of Petroleum (East China). His research interests include seismic wave forward propagation and imaging. He has won several honors, including the Outstanding Graduate Student Instructor and the second prize of Science and Technology Progress in Shandong, China.

MIN ZHANG received the B.S. degree in computer science and the M.S. and Ph.D. degrees in geophysics from the China University of Petroleum (East China), Qingdao, China, in 2005, 2007, and 2011, respectively, and the Joint Training Ph.D. in geophysics from UT–Austin, Austin, USA.

Since 2011, she has been a Senior Experimentalist with the School of Geoscience, China University of Petroleum (East China). Her research interests include illumination analysis and observation system optimization, seismic data denoising, seismic wave propagation and imaging, velocity inversion and modeling, and time-lapse seismic data processing. She has won the Excellent Instructor Award many times in the National Undergraduate Exploration Geophysics Competitions.

YIXUAN GAO is currently pursuing the B.S. degree in biological science with Qufu Normal University.

Her research interests include swarm intelligence and deep learning.

WANYUE GAO is currently pursuing the B.S. degree in logistics with Shandong Normal University.

Her research interests include supply chain management and deep learning.